

SPATIALLY RESOLVED STELLAR KINEMATICS OF FIELD EARLY-TYPE GALAXIES AT $Z = 1$: EVOLUTION OF THE ROTATION RATE ¹

ARJEN VAN DER WEL² & ROELAND P. VAN DER MAREL³
The Astrophysical Journal, Accepted

ABSTRACT

We use the spatial information of our previously published VLT/FORS2 absorption line spectroscopy to measure mean stellar velocity and velocity dispersion profiles of 25 field early-type galaxies at a median redshift $z = 0.97$ (full range $0.6 < z < 1.2$). This provides the first detailed study of early-type galaxy rotation at these redshifts. From surface brightness profiles from HST imaging we calculate two-integral oblate axisymmetric Jeans equation models for the observed kinematics. Fits to the data yield for each galaxy the degree of rotational support and the mass-to-light ratio M/L_{Jeans} . S0 and Sa galaxies are generally rotationally supported, whereas elliptical galaxies rotate less rapidly or not at all. Down to $M_B = -19.5$ (corrected for luminosity evolution), we find no evidence for evolution in the fraction of rotating early-type (E+S0) galaxies between $z \sim 1$ ($63\% \pm 11\%$) and the present ($61\% \pm 5\%$). We interpret this as evidence for little or no change in the field S0 fraction with redshift. We compare M/L_{Jeans} with M/L_{vir} inferred from the virial theorem and globally averaged quantities, and assuming homologous evolution. There is good agreement for non-rotating (mostly E) galaxies. However, for rotationally supported galaxies (mostly S0) M/L_{Jeans} is on average $\sim 40\%$ higher than M/L_{vir} . We discuss possible explanations and the implications for the evolution of M/L between $z = 1$ and the present, and its dependence on mass.

Subject headings: galaxies: elliptical and lenticular, cD—galaxies: kinematics and dynamics—galaxies: evolution—galaxies: fundamental parameters

1. INTRODUCTION

Detailed studies of nearby early-type galaxies provide insight into their stellar populations, dark matter content and kinematic and spatial structure. In particular, resolved kinematic data reveal the underlying gravitational potential (e.g., van der Marel 1991; Cappellari et al. 2006), the presence of super-massive black holes (e.g., Richstone et al. 1990; Verolme et al. 2002) and dark halos (e.g., Kronawitter et al. 2000), and the relative contributions of pressure and rotation to its orbital energy (e.g., Binney 1978; Davies et al. 1983; Emsellem et al. 2007).

Recently, the first, probing steps have been made towards spatially resolving the stellar motions in more distant early-type galaxies using absorption-line spectroscopy. The past few years have seen studies aimed at constraining the dark halos of lensing galaxies (Koopmans et al. 2006), dynamically distinguishing cluster E and S0 galaxies (Moran et al. 2007), constraining the evolution in rotation rate (van der Marel & van Dokkum 2007a), and constraining the evolution of the mass-to-light ratio (M/L) using the M/L vs. σ relation at intermediate redshift (van der Marel & van Dokkum 2007b). Obviously, the spatial resolution and errors in the kinematic quantities

are much larger than for local galaxies, and consequently, the level of detail is far lower. Still, the spatially resolved information that is obtained by going beyond studies of global quantities alone, combined with the addition of cosmic time to the equation, have already revealed several interesting results.

Moran et al. (2007) used rotation curves to address the question whether E and S0 galaxies are coeval or not. They found that the relative number of rotationally supported early-type galaxies at $z \sim 0.5$ is lower than today, especially in clusters. Combined with extensive studies of visually classified samples of galaxies out to $z \sim 1$ (Dressler et al. 1997; Postman et al. 2005; Smith et al. 2005), this is the best evidence to date for relatively recent S0 formation, presumably through the transformation of in-falling, star-forming Sa-like galaxies into quiescent cluster S0 galaxies (e.g., Gunn & Gott 1972; Larson et al. 1980).

This classical picture does not address the high fraction of S0 galaxies at low densities. Approximately 60% of all early-type galaxies in the field are S0 galaxies. Moreover, recently it was shown that the total fraction of early-type galaxies does not significantly change between $z \sim 0.8$ and the present in either clusters (Holden et al. 2007) or in the field (van der Wel et al. 2007) if only galaxies with masses $M \gtrsim 0.5M^*$ are considered. This calls into question the claim that S0 galaxies evolve differently from E galaxies, although we note this has so far not been explicitly addressed. Because of these reasons it is important to not lose sight of alternative scenarios for the formation of S0 galaxies. Merging that does not completely destroy the disk is another proposed mechanism (e.g., Bekki 1997). This is more similar to the favored formation mechanism for E galaxies, and would therefore

¹ Based on observations collected at the European Southern Observatory, Chile (169.A-0458) and on observations with the *Hubble Space Telescope*, obtained at the Space Telescope Science Institute, which is operated by AURA, Inc., under NASA contract NAS 5-26555.

² Department of Physics and Astronomy, Johns Hopkins University, 3400 North Charles Street, Baltimore, MD 21218; e-mail: wel@pha.jhu.edu

³ Space Telescope Science Institute, 3700 San Martin Drive, Baltimore 21218

imply that E and S0 are in fact one class of objects with a large range in bulge-to-disk ratios. This ratio may be related to the mass ratio and the dissipation of the mergers (e.g., Naab et al. 2006a). In this scenario E and S0 galaxies are expected to be roughly coeval.

Another interesting observation in these contexts is that van der Marel & van Dokkum (2007a) found some evidence that the relative number of rotationally supported cluster elliptical galaxies decreases slightly between $z \sim 0.5$ and the present. This points toward a scenario in which elliptical galaxies gradually lose angular momentum through interactions and mergers (e.g., Naab et al. 2006b). This result is not necessarily inconsistent with the conclusions from Moran et al. (2007). The latter authors used rotation to trace the number of S0 galaxies, whereas the sample of van der Marel & van Dokkum (2007a) contained (almost) no S0 galaxies by construction. Therefore, these studies probed different aspects of the early-type (E+S0) galaxy population.

Besides constraining rotation, resolved kinematic data also allow for a measurement of M/L . The evolution of M/L with redshift is typically studied using estimates based on the virial theorem or the fundamental plane (e.g., van Dokkum & van der Marel 2007). This uses only globally averaged quantities (luminosity, radius, integrated velocity dispersion), combined with assumptions about the dynamical structure of the galaxies and the homology of their evolution. Spatially resolved kinematics have the advantage that they allow the M/L to be inferred through detailed dynamical modeling, which removes some of the assumptions inherent in these studies. Systematic effects may affect not only the measured, average evolution of M/L , but also the evolution of the tilt of the fundamental plane, i.e., the dependence of M/L evolution on galaxy mass (e.g., van der Wel et al. 2005; Treu et al. 2005). van der Marel & van Dokkum (2007b) addressed this for a sample of cluster ellipticals at $z \sim 0.5$. They found that bright, non-rotating galaxies are consistent with homologous evolution, but that the situation may be more complicated for less-luminous, rotating galaxies. However, the small size of their sample and the limited number of S0 galaxies left room for different interpretations of this result.

In this paper we study the resolved kinematics of a sample of field early-type galaxies at $z \sim 1$, using spatially resolved spectra from the *Very Large Telescope* (VLT) and imaging from the *Hubble Space Telescope* (HST). This dataset was presented earlier by van der Wel et al. (2005). Our analysis methodology is largely similar to that of van der Marel & van Dokkum (2007a,b). However, our sample is different from theirs in three important areas. First, we focus on field galaxies instead of cluster galaxies. Second, our sample includes significant numbers of S0 and Sa galaxies, instead of just E galaxies. And third, we work at $z \sim 1$ instead of $z \sim 0.5$, thus providing a much extended baseline for studying evolution. In particular, we quantify the evolution of the relative number of rotationally supported field early-type galaxies from $z \sim 1$ to the present, and examine the difference between the M/L inferred from spatially resolved and unresolved kinematic data.

We have organized the paper as follows. In Section 2 we introduce the data. In Section 3 we briefly describe

the dynamical modeling. In Section 4 we present our results regarding rotational support. In Section 5 we present our results regarding the M/L . In Section 6 we summarize the main conclusions. We adopt the following cosmological parameters: $(\Omega_M, \Omega_\Lambda, h) = (0.3, 0.7, 0.7)$.

2. DATA

2.1. Spectroscopy

Very deep VLT/FORS2 spectroscopy of a sample of magnitude-limited, morphologically selected field early-type galaxies at redshifts $0.6 < z < 1.2$ in the Chandra Deep Field-South (CDF-S) and the foreground of the $z = 1.24$ cluster RDCS 1252.9-2927 (CL1252) were presented by van der Wel et al. (2005). That paper provides a full description of the data reduction, including the technique used to measure the global velocity dispersion of each galaxy from its absorption features. In this paper we examine a subsample of 25 early-type galaxies (10 E, 9 S0, and 6 Sa galaxies) that have such high-quality spectra that variations of mean velocity v and velocity dispersion σ along the slit can be measured. The median redshift of this subsample is $z = 0.97$. Since this is a magnitude-limited subsample it is not biased against rotating or non-rotating galaxies, and it is representative for the entire population of E+S0 galaxies at this redshift.

For high-redshift galaxies, σ is usually determined from an extracted spectrum that is averaged over multiple pixels in the spatial direction in order to optimize for signal-to-noise ratio (S/N). Here, instead, we measure v and σ for each individual row of pixels ($0''.25$ long) for which the S/N is sufficiently high for a robust measurement. We use the same wavelength range and template stars as used by van der Wel et al. (2005) such that differences between the results from averaged and resolved spectra are solely due to differences in the observed spectra themselves. The mean velocity profiles, typically measured for 5–7 pixel rows, are shown in Figure 1. It is readily apparent that many galaxies show signs of significant rotation. Measuring σ requires better S/N , therefore σ can usually only be measured for 3–5 pixel rows. The S/N is typically 15 \AA^{-1} for the outermost pixel rows for which we measure σ (the central pixel rows obviously have the highest S/N). For two galaxies (CDF-S-18 and CDF-S-23) we only have $S/N < 8 \text{ \AA}^{-1}$ for the outermost pixel rows, which is not ideal for velocity dispersion measurements. However, for consistency we retained these rows in our analysis because the large resulting error bars are explicitly accounted for in our modeling described in Section 3. In Figure 2 we show the σ profiles. In both Figures 1 and 2 we over-plot the best-fitting models that we describe in Section 3 below.

2.2. Photometry

GOODS⁴ provides deep, publicly available HST/ACS imaging of the CDF-S (Giavalisco et al. 2004). ACS imaging for the field of CL1252 is also available (Blakeslee et al. 2003). We used these data to assign morphological classifications (E; S0; Sa) based on visual inspection of the images, following the strategy outlined

⁴ <http://www.stsci.edu/science/goods/>

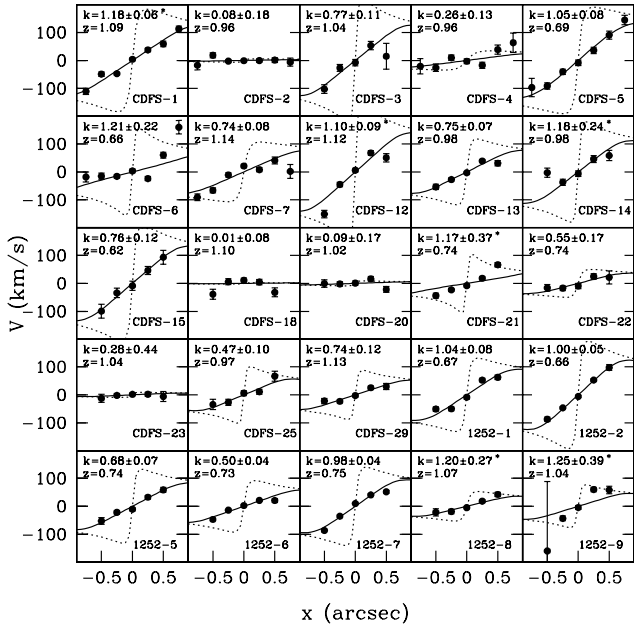


FIG. 1.— Profiles of mean velocity v for 25 field early-type galaxies at redshifts $0.6 < z < 1.2$. The points indicate the measured velocity at each spatial pixel in the spectroscopic slits. The solid curves show the predictions of the best-fitting models. For comparison, dotted curves are the corresponding predictions when seeing convolution and pixel/slit binning are not taken into account. The visual morphology, the redshift, and the inferred rotation parameter k are given for each object. An asterisk indicates that the maximum value for k that is physically possible is adopted instead of the best-fitting value for k . The ID numbers correspond to those given in van der Wel et al. (2005) where more information regarding the photometric and kinematic properties can be found.

by Postman et al. (2005). These classifications are used throughout this paper.

van der Wel et al. (2005) used the F850LP images to fit de Vaucouleurs profiles to the objects in their sample in order to determine their effective radii R_{eff} and surface brightnesses μ_{eff} . For the present analysis we use the ACS data to measure the full surface brightness profile for each galaxy. We follow the same procedure described by van der Marel & van Dokkum (2007a). First, the images are deconvolved with the point-spread function (PSF, for which we use stars in the field) using the Lucy-Robertson algorithm. Subsequently, we fit elliptical isophotes to the two-dimensional images with the IRAF task ‘ellipse’. This yields one-dimensional profiles of major axis surface brightness, position angle, and ellipticity. For galaxies at redshifts $z > 0.85$ we use the ACS F850LP images and for galaxies at redshifts $z < 0.85$ we use the ACS F775W images. With these choices, the observed wavelength corresponds as closely as possible to the rest-frame B -band. The observed surface brightness profiles are transformed into the rest-frame B -band using the method presented in van Dokkum & van der Marel (2007). This facilitates the comparison with local galaxy samples.

3. MODELS

For a full description of the modeling procedure we refer to van der Marel & van Dokkum (2007a). In short, the rest-frame B -band photometry described in Section 2.2 is fitted with the projection of a parameter-

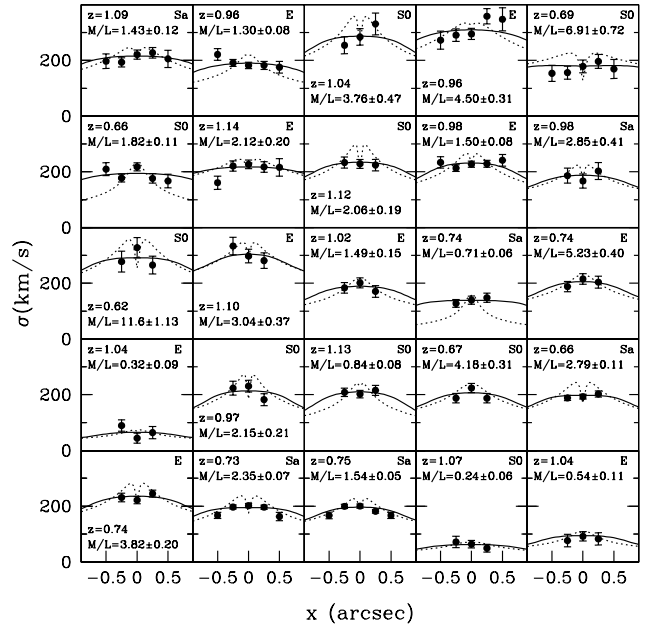


FIG. 2.— Profiles of velocity dispersion σ for the same 25 field early-type galaxies at redshifts $0.6 < z < 1.2$ as in Figure 1. The points indicate the measured dispersion at each spatial pixel in the spectroscopic slits. The solid curves show the predictions of the best-fitting models. For comparison, dotted curves are the corresponding predictions when seeing convolution and pixel/slit binning are not taken into account. The visual morphology, the redshift, and the rest-frame B -band model M/L in solar units are given for each object.

ized, oblate axisymmetric, constant axial-ratio luminosity distribution. The results of the modeling are fairly insensitive to variations in the unknown inclination (van der Marel & van Dokkum 2007a,b). In the discussion below we adopt for each galaxy the inclination angle that is most likely, given the probability distribution of intrinsic axial ratios derived from large galaxy catalogs of the local universe.

Given the three-dimensional luminosity density, the Jeans equations are solved under the assumptions of a constant M/L and a two-integral distribution function $f = f(E, L_z)$, where E is the energy and L_z the angular momentum around the symmetry axis. The models have $\overline{v_R^2} \equiv \overline{v_z^2}$, so their velocity distribution is isotropic in the meridional plane. The ratio of $\overline{v_\phi^2}$ to $\overline{v_R^2}$ is determined by the requirement of hydrostatic equilibrium. The second azimuthal velocity moment is split into mean and random components according to the convenient parameterization

$$\overline{v_\phi} = k[\overline{v_\phi^2} - \overline{v_R^2}]^{1/2}. \quad (1)$$

A value $k = 0$ yields a galaxy that is non-rotating and fully pressure supported. A value $|k| = 1$ yields an oblate isotropic rotator, i.e., a galaxy with sufficient rotation to fully explain its flattening. $|k|$ can be larger than unity, with a physical maximum that depends on the shape of the galaxy, and set by the requirement that $\sigma_\phi^2 \equiv \overline{v_\phi^2} - (\overline{v_\phi})^2$ is everywhere positive. In the following we always choose the major axis position angle (which is indeterminate module 180 degrees) so that k is positive.

The solutions of the Jeans equations are integrated

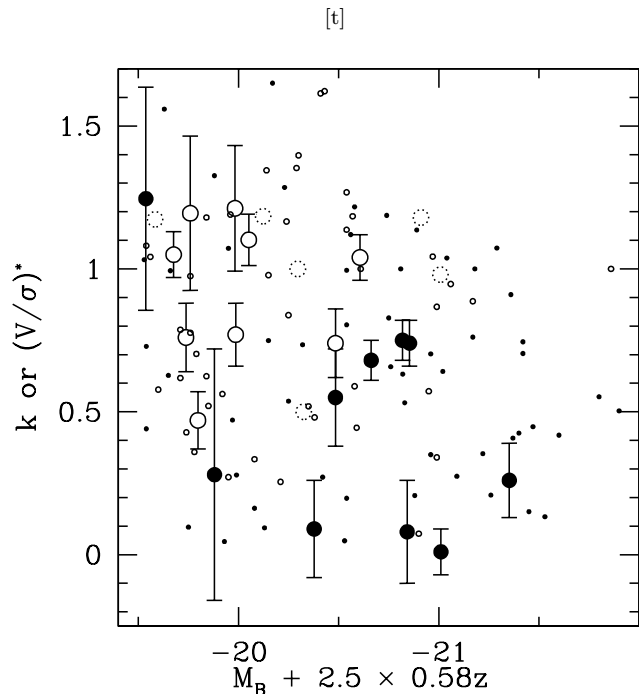


FIG. 3.— B -band luminosity vs. rotation rate. The large symbols are the 25 field early-type galaxies at redshifts $0.6 < z < 1.2$, for which we show the rotation parameter k . The luminosities are corrected for 0.58 dex of evolution between $z = 1$ and the present (van Dokkum & van der Marel 2007). Filled symbols are E galaxies, open circles are S0 galaxies, and open, dotted circles without error bars are Sa galaxies, as determined by visual classification. The local comparison sample is shown as small symbols, with the different morphologies distinguished by the same symbols as used for the distant sample. $(V/\sigma)^*$, which is comparable to k , is used to quantify the rotation rate for the local galaxy sample. The distributions of the local and distant samples are similar.

along the line of sight, and then convolved in luminosity-weighted sense with the seeing (typically $0''.6 - 0''.8$) and with the size of the pixels ($0''.25$ long) in the slit ($1''.0$ wide) through which the galaxies' spectra were taken, taking the angle between the orientation of the slit and the major axis into account. The match of the predictions to the kinematic data from Section 2.1 is optimized by finding the best-fitting value of the two available model parameters. The mass-to-light ratio M/L determines the total amount of RMS motion ($\sqrt{v^2 + \sigma^2}$) whereas the parameter k determines the amount of rotational support (which is related to v/σ). Solid curves in Figures 1 and 2 show the best model fits. For comparison, dotted curves show the model predictions if no account is taken of seeing and pixel/slit-binning. Clearly, the latter makes a considerable difference and it is therefore important that this is properly modeled. Best-fit values of k are listed in the individual panels of Figure 1.

4. ROTATION AT $Z \sim 1$

4.1. Evolution in Rotation Rate

As is readily apparent from Figure 1, many early types at $z \sim 1$ show signs of rotation. In Figure 3 we show using large symbols the rotation parameter k as a function of absolute B -band magnitude, distinguishing between galaxies with different visual morphologies. The absolute magnitudes are corrected for luminosity evolution using the results of van Dokkum & van der Marel

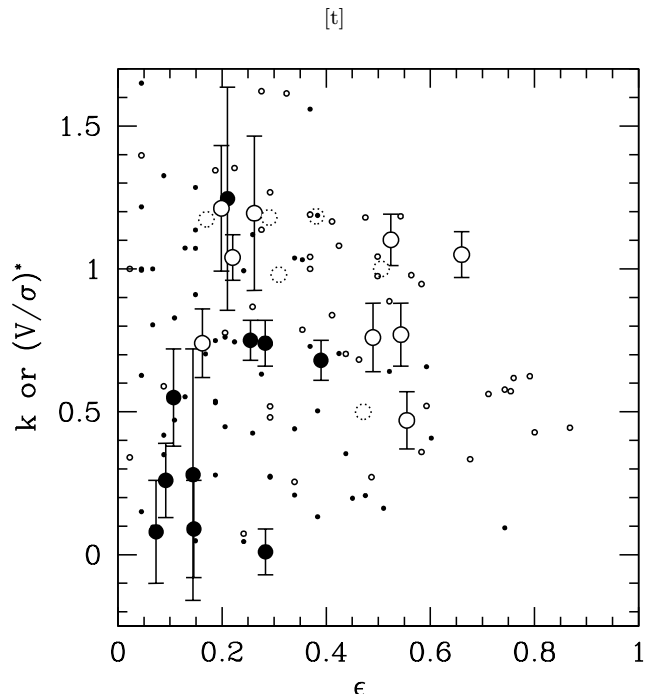


FIG. 4.— Ellipticity vs. rotation rate (k for the distant sample, $(V/\sigma)^*$ for the local sample). The symbols that indicate different visual classifications are the same as in Figure 3. The ellipticity distribution, like the rotation rate distribution, is similar for the local and distant samples.

(2007). Slightly different values would have been reasonable as well (see, e.g., Section 5.2), but none of our results depend sensitively on this.

Only 5 out of the 25 galaxies show little or no rotation. These are all ellipticals. By contrast, all S0 and Sa galaxies show significant rotation, with many consistent with being rotationally supported. Figure 4 shows the rotation parameter k as a function of the apparent ellipticity $\epsilon \equiv 1 - (b/a)$, using similar symbols as in Figure 3. This shows that the non-rotating galaxies tend to be rounder than most of the rotating galaxies.

As noted by Moran et al. (2007), a single-component, spheroidal model may not be representative for S0 galaxies, some of which clearly show disks. Our models can in principle be extended to include disks (Cinzano & van der Marel 1994), but we have not explored that here. Therefore, the inferred k may not always necessarily correspond to the physical property it represents in the model. Nonetheless, as fit parameter, k still provides an effective measure of the relative importance of rotation in the galaxy. In fact, Figures 3 and 4 show that E and S0 galaxies can be distinguished fairly successfully based on their kinematics, as quantified by the parameter k . Additional use of luminosity and axial ratio information can further increase the accuracy of such a kinematical classification scheme, as advocated by Moran et al. (2007). The only galaxy that seems somewhat out of place in Figure 3 is the most rapidly rotating elliptical galaxy. However, this is also the least luminous galaxy in the sample, and it may well have been visually misclassified.

The clean kinematic separation between different morphological types at $z \sim 1$ is surprising given the complex situation for local early-type galaxies (Emsellem et al.

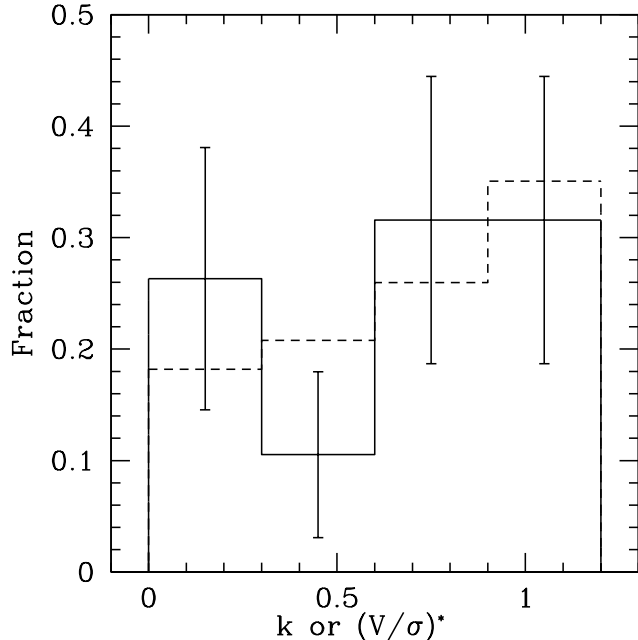


FIG. 5.— Histograms of early-type (E+S0) galaxy rotation rates. The parameter k is used for the distant sample (solid line with Poisson error bars) and the quantity $(V/\sigma)^*$ is used for the local sample (dashed line). Only galaxies brighter than $M_B = -19.5$ are included (corrected for luminosity evolution, in the case of the distant sample). There is no significant difference between the two samples in terms of relative numbers of slow-rotating and fast-rotating galaxies.

2007). Both E and S0 galaxies are often fast rotators with overlapping kinematic properties (Cappellari et al. 2007). The clean separation at higher redshifts is therefore quite likely partially artificial. Morphological classifications are difficult at high redshift, and recent work has shown that the relative number of S0 galaxies at high redshift is systematically underestimated as evidenced by the lack of S0 galaxies with $\epsilon < 0.3$ (Holden et al, submitted). In addition, elongated, rotating elliptical galaxies can be mis-classified as S0 galaxies. Nonetheless, these concerns are not relevant for the main goal of this paper, the evolution of the rotation of early-type galaxies as a single class of objects.

To address the issue of evolution in the rotation rate, we compare the $z \sim 1$ sample with a local sample extracted from the Lyon Extragalactic DataBase (LEDa; Paturel et al. 1997), which is distributed and made available as HyperLeda (Paturel et al. 2003)⁵. We restrict the local sample to galaxies within ~ 40 Mpc (distance modulus $m - M < 33$). In order to construct a field/group E+S0 sample we only included galaxies with less than 80 neighbors brighter than $M_B = -19.5$ within a cylinder with a 5 Mpc diameter (at the distance of the galaxy) and with a difference in radial velocity with respect to the cosmic microwave background of less than 1000 km s^{-1} . This effectively selects a complete sample of 179 galaxies (70 Es; 109 S0s) outside over-dense structures (most notably, the Virgo cluster). The median projected surface density is $\Sigma = 0.4 \text{ Mpc}^{-2}$, which is derived from the distance to the 7th nearest neighbor down to the

luminosity limit of the magnitude-limited sample with the same radial velocity within 1000 km s^{-1} . This is the same value as for a large, volume-limited sample of galaxies at $z \sim 0.03$ (see van der Wel et al. 2007). It is also comparable with the estimated surface density (in co-moving units) for a sample of distant field galaxies (see van der Wel et al. 2007) of which our distant sample is a sub-sample. Maximum stellar velocities V and velocity dispersions σ are known for 55 Es and 43 S0s (Prugniel & Simien 1996). There are 37 galaxies in this sample for which multiple, independent measurements of the rotation velocity V are available. For 31 of these the measurements are consistent within the errors. The measurements are inconsistent only for the remaining 6 (see Table A2 of Prugniel & Simien 1996). Because especially galaxies with peculiar properties tend to be targeted multiple times, the measurements for the remainder of the sample may actually be even better. Therefore, the kinematic measurements for the local sample are generally reliable and reproducible.

We quantify the rotation rate of the local sample using the quantity $(V/\sigma)^* = (V/\sigma)\sqrt{(1-\epsilon)/\epsilon}$. This approximates the ratio of the actual rotation rate of the galaxy to the ratio expected for an oblate isotropic rotator of the given observed axial ratio (Davies et al. 1983). This quantity is therefore similar to our model parameter k . The only difference is that k is defined locally in the meridional plane by equation (1), whereas $(V/\sigma)^*$ is defined in terms of the globally defined projected quantities V , σ and ϵ . van der Marel (1991, see his Figure 3a) made a direct comparison of k and $(V/\sigma)^*$ for a sample of local galaxies, and found a good agreement to $\sim 10\%$. For the present paper we therefore compare $(V/\sigma)^*$ for the local sample directly to k for the distant sample.

The local sample is shown in Figures 3 and 4 using small symbols. As compared to the distant sample, there are some differences in the types of galaxies that show high rotation rates. In the distant sample these are almost all flattened, visually classified S0 galaxies. By contrast, in the local sample these include quite a few roundish, visually classified E galaxies. It has been known for some time (e.g., Rix & White 1990) that local galaxy catalogs are deficient in such galaxies. Of course, distant samples may be plagued by similar, or worse, problems. However, our sample size is too small to make definite statements about this issue.

As noted earlier, possible uncertainties in the relative classifications of E and S0 galaxies do not affect the assessment of the rotation rate distribution of early-type (E+S0) galaxies in general. Figure 5 shows that the rotation rate histograms are statistically indistinguishable for the local and distant samples. $63 \pm 11\%$ (12 out of 19) of the E+S0 galaxies in the distant sample have high rotation rates ($k > 0.6$), and $59 \pm 5\%$ (58 out of 98) of those in the local sample have high rotation rates ($(V/\sigma)^* > 0.6$).

The similarity between these two numbers is striking, however, they may not be directly comparable as the kinematic data for the local sample are not complete, nor representative for the morphological composition of the population: an E galaxy is twice as likely to have kinematic data than an S0 galaxy (see numbers above). If we, very crudely, assume that all S0 galaxies rotate and

⁵ <http://leda.univ-lyon1.fr>

all E galaxies do not, then the fraction of rotating E+S0 galaxies would be 69%. However, in reality the relative fractions of rotating/non-rotating E and S0 galaxies are not very different (55% and 65%, respectively, see the small data points in Figure 3). Based on these relative numbers of rotating galaxies for E and S0 galaxies as separate classes we estimate that the true relative fraction of rotating early-type galaxies is 61%, only slightly higher than the measured value of 59%.

Concluding, we find no evidence for evolution in the rotation rate of field early-type galaxies between $z = 1$ and the present down to the luminosity limit of the distant sample, $M_B = -19.5$. The distant sample is small (as evidenced by the large error bars in Figure 5), but we would have detected an increase or decrease by more than 25% in the relative number of rotating galaxies if there were such evolution.

4.2. Comparison With Previous Results

The only previous measurement of the evolution of the relative number of rotationally supported early-type (E+S0) galaxies is that of Moran et al. (2007). Those authors found substantial evolution for cluster early-type galaxies in the sense that fewer early-type galaxies are rotationally supported at $z \sim 0.5$ than locally, which is interpreted as evidence for a lower S0 fraction in the distant clusters. This result for cluster galaxies is not directly comparable to ours. However, the *field* early-type galaxy sample from Moran et al. (2007) contains only $43\% \pm 14\%$ rotating galaxies, which is less than the value for local galaxies inferred from the LEDA sample described above. If this (marginally significant) decrease between $z \sim 0.5$ and the present is real, more evolution between $z \sim 1$ and the present can be expected, but in our sample we do not observe this. Besides the low significance, this comparison is furthermore hampered by differences in methodology. Therefore it is interesting to compare our results and methods with those from Moran et al. (2007) in more detail.

Both we and Moran et al. (2007) measured spatially resolved kinematical profiles of galaxies, but beyond that our methods are very different. Moran et al. (2007) infer global quantities (the rotation v , velocity dispersion σ , and ellipticity), and they do so directly from the data. Observational effects are not taken into account, and the internal dynamics of the galaxies are not modeled. Our method aims to model the internal dynamics, to take into account known differences between galaxies (e.g., in their surface brightness profile), and to account explicitly for all known observational influences on the measured quantities. The approach of Moran et al. (2007) has the advantage of being simple and model-independent. However, ignoring the effects of seeing convolution and pixel/slit binning can bias the results. Figure 1 shows that these effects have a significant impact on both the measured rotation value at the outermost radius and the maximum value of the rotation curve. As a result, the relative number of rotating galaxies can be underestimated.

To quantitatively illustrate the effect of seeing convolution and pixel/slit binning, we apply one of the kinematic classifiers of Moran et al. (2007), namely $v/(1-\epsilon)$, to our datasets. Here, v is defined as half the velocity range of a fitted straight line from end to end of the

measured velocity profile, approximating the maximum rotation velocity. From the LEDA sample we derive that $65\% \pm 5\%$ of the local population satisfy the criterion from Moran et al. (2007), virtually the same fraction as galaxies with $(V/\sigma)^* > 0.6$ (see Section 4.1). This demonstrates that for the purpose of distinguishing rotating and non-rotating galaxies, the two methods are in principle comparable.

In our $z \sim 1$ sample only 7 out of 19 E+S0 galaxies ($37 \pm 11\%$) have $v/(1-\epsilon) > 85 \text{ km s}^{-1}$, consistent with the results from Moran et al. (2007) for $z \sim 0.5$ field galaxies, but substantially less than the number of galaxies with $k > 0.6$ ($63 \pm 11\%$) in our $z \sim 1$ field sample. However, if we use the maximum model line-of-sight velocity, with observational effects taken into account (i.e., the dotted curves instead of the solid curves in Figure 1), then we find a higher fraction with $v/(1-\epsilon) > 85 \text{ km s}^{-1}$: $63 \pm 11\%$, the same as the fraction of galaxies with $k > 0.6$. This implies that omission of the effects of seeing convolution and pixel/slit binning can lead to significant underestimates of the number of rotating galaxies at high redshift. This may well explain the relatively low number of kinematically classified field S0 galaxies found by Moran et al. (2007) at $z \sim 0.5$. However, we cannot assess the question to what extent the above described bias contributes to the evolution that Moran et al. (2007) found for cluster galaxies.

Interestingly, the kinematic classifications by Moran et al. (2007) agree, statistically speaking, with visual morphological classifications, both at low and at high redshift. This either argues against a bias in their results, or that visual classifications can suffer from a similar bias against rotating/S0 galaxies. An indication that high- z classifications of S0 galaxies are indeed hampered by systematic problems is that the ellipticity distribution for the cluster early-type galaxy population does not change significantly with redshift, suggesting that high- z S0 galaxies are systematically misclassified as E galaxies, more so than the other way around (Holden et al., in prep.). Still, to what extent biases contribute to an apparent decline in the S0 fraction with redshift will probably continue to be a matter of debate for some time to come. Also, the answer may well be different for cluster and field galaxies. However, it is certainly intriguing that our detailed observations and modeling of field galaxies at $z \sim 1$ show no evolution in the fraction of rotating early-type galaxies.

Note that our result does not necessarily imply that there is no evolution in the early-type galaxy population. On the one hand, rotationally supported early-type galaxies may merge, and produce pressure-supported elliptical galaxies (e.g., Naab et al. 2006b). This process would produce an increase in the fraction of elongated/rotating galaxies with redshift, for which some tentative evidence exists in clusters from the results of van der Marel & van Dokkum (2007a). On the other hand, rotating, quiescent galaxies may be formed out of Sa galaxies that cease to form stars, contributing to the increase in the stellar mass density of red galaxies (e.g., Bell et al. 2004; Brown et al. 2007), and the decrease of the cosmic average star formation rate (e.g., Le Floch et al. 2005; Noeske et al. 2007). As long as the mechanisms that increase and decrease the relative num-

bers of rotating and non-rotating galaxies do not change their ratio, continued growth of both the E and the S0 population is possible up to the present day.

The results of neither our own study nor that of Moran et al. (2007) are directly comparable to those obtained by van der Marel & van Dokkum (2007a) using the same technique as was in this paper. This is because their study at $z \sim 0.5$ dealt with a cluster sample that was preselected to contain almost no S0 galaxies. Therefore, it can shed little light on the evolution of the S0 fraction with redshift.

5. MASS-TO-LIGHT RATIOS

5.1. Comparison between Model and Virial M/L Estimates

According to the virial theorem, the mass of a stellar system can be written as

$$M_{\text{vir}} = \frac{\beta R_{\text{eff}} \sigma_{\text{eff}}^2}{G}, \quad (2)$$

where R_{eff} is the effective radius and σ_{eff} is the luminosity-weighted velocity dispersion measured through an aperture of size R_{eff} . The homology parameter β generally depends on the detailed density structure and velocity dispersion anisotropy of the galaxy. Plausible models can span a wide range of β values. However, Cappellari et al. (2006) found that early-type galaxies in the local universe all follow $\beta = 5.0 \pm 0.1$, with surprisingly low scatter. This calibration was obtained by calculating galaxy masses M from detailed dynamical models for integral-field kinematical data, including higher-order velocity moments. The quantity σ_{eff} was measured by integration over the spatially resolved two-dimensional velocity field. The virial mass-to-light ratio M/L_{vir} can be calculated upon division by the luminosity L . The latter can be measured through aperture photometry or it can be estimated as $L = 2\pi R_{\text{eff}}^2 I_{\text{eff}}$, where I_{eff} is the average intensity inside of R_{eff} .

Equation (2) is commonly used to estimate the mass of distant galaxies. In doing so, one generally measures the velocity dispersion σ_c through a spectroscopic aperture. The velocity dispersion σ_{eff} is then estimated by applying a correction formula that is based on typical observations of local galaxies (Jørgensen et al. 1995). However, the findings of Cappellari et al. (2006) do not guarantee that equation (2) with $\beta = 5$ is as accurate as it is in the local universe, for at least two different reasons. First, galaxies may evolve so that the homology parameter β could be a function of redshift. Second, the accuracy and applicability of the corrections from σ_c to σ_{eff} is not guaranteed at high redshift. The spectroscopic apertures and the seeing in use there often exceed the galaxy size R_{eff} . Observations that adequately mimic this are not available in the local universe. Moreover, even in the local universe $\sigma_{\text{eff}}/\sigma_c$ shows strong variations from galaxy to galaxy (Cappellari et al. 2006). It is therefore necessary to calibrate equation (2), and the appropriate value of β , at high redshift in the same way as was done locally. This is possible for our sample by comparing the M/L_{Jeans} from our dynamical models (Section 3) with the values of M/L_{vir} . Our data quality is obviously not comparable to the two-dimensional velocity fields and higher-order moments that are available locally. Nonetheless,

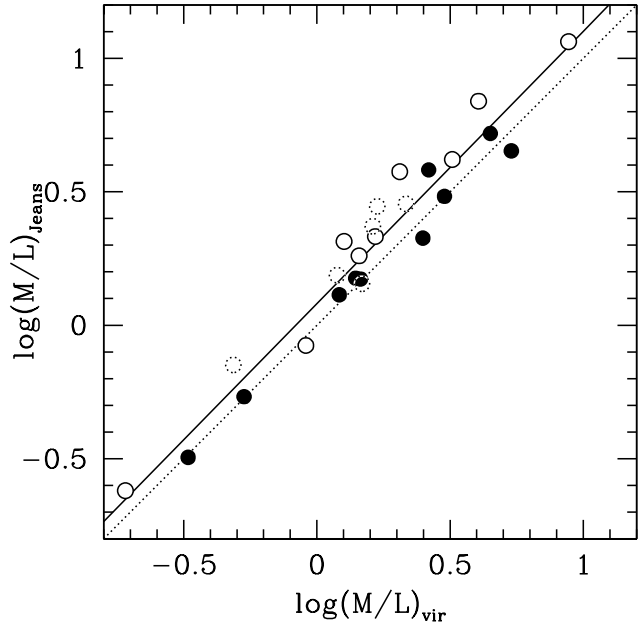


FIG. 6.— Jeans M/L vs. virial M/L (calculated using $\beta = 5$ in eq. [2]) for the $z \sim 1$ galaxy sample. The symbols that indicate different visual classifications are the same as in Figure 3. E galaxies follow the relation $M/L_{\text{Jeans}} \approx M/L_{\text{vir}}$ (dotted line). However, S0 galaxies on average have M/L_{Jeans} systematically higher than M/L_{vir} by $\sim 40\%$. The solid line is the least-squares fit for the full sample, which has $M/L_{\text{Jeans}} \propto M/L_{\text{vir}}^{1.02}$ (and has M/L_{Jeans} systematically higher than M/L_{vir} by $\sim 20\%$).

this calibration is unique and has not previously been done at these redshifts.

In Figure 6 we compare M/L_{vir} and M/L_{Jeans} for our sample at $z \sim 1$. We computed M/L_{vir} using $\beta = 5$, with σ_c and R_{eff} as measured by van der Wel et al. (2005). The spectroscopic aperture was defined by the width of the spectroscopic slit ($1''$) and the height of the extracted spectrum (usually, $1.25''$). The ratio $\sigma_{\text{eff}}/\sigma_c$ was estimated using the formula of Cappellari et al. (2006), which is consistent with those of Jørgensen et al. (1995). As for local galaxies, the slope of the best-fitting linear relation between M/L_{vir} and M/L_{Jeans} is consistent with unity. However, there is a systematic offset that appears to depend on the galaxy type. This is seen in the residuals $\log[(M/L)_{\text{Jeans}}/(M/L)_{\text{vir}}]$ shown in Figure 7. For E galaxies, the residuals are consistent with zero. Therefore, $\beta = 5$ is appropriate for E galaxies at high redshift, and as a class E galaxies are consistent with homologous evolution. For S0 (and Sa) galaxies, on the other hand, M/L_{Jeans} is on average almost 40% higher than M/L_{vir} . As shown in Figures 7a,b, these galaxies tend to be flatter and more-rapidly rotating than the E galaxies. These results are consistent with the earlier findings of van der Marel & van Dokkum (2007b) in clusters at $z \sim 0.5$. However, the trends are much clearer in the present sample because of its higher fraction of rapidly rotating S0 and Sa galaxies.

There are several possible explanations for the trends observed in Figure 7. First, S0 and Sa galaxies at $z \sim 1$ may have $\beta > 5$. However, this would imply that these galaxies evolve non-homologously, while E galaxies do not. This seems to us unlikely as in that case it would

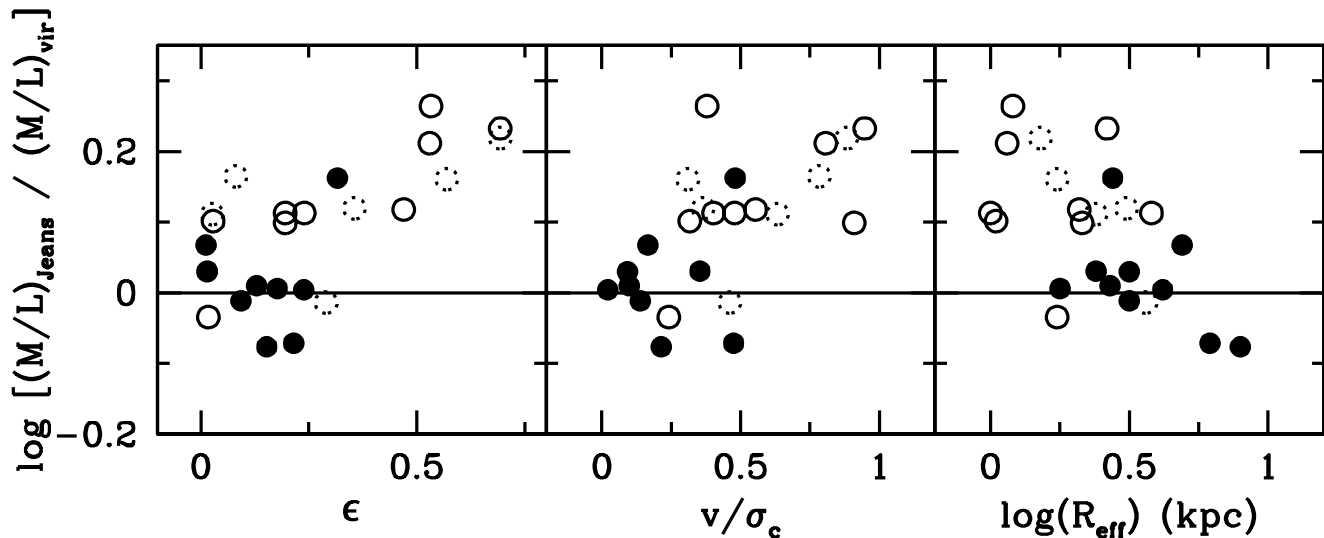


FIG. 7.— The logarithm of the ratio $(M/L)_{\text{Jeans}}/(M/L)_{\text{vir}}$ vs. ellipticity (*left panel*), v/σ with v as defined by Moran et al. (2007) (*middle panel*), and effective radius (*right panel*). The symbols that indicate different visual classifications are the same as in Figure 3. The residuals tend to be positive for galaxies of S0 or Sa type, for galaxies with significant ellipticity or rotation rate, or for galaxies of small size. Possible causes for this, and implications for studies of fundamental plane evolution, are discussed in the text.

be an odd coincidence that $\beta = 5$ for all types of local galaxies. Second, it is possible that our models have overestimated the M/L_{Jeans} for rapidly rotating galaxies. Such galaxies may have rapidly rotating disks that are not well represented by our constant axial ratio oblate models. However, Cinzano & van der Marel (1994) addressed this issue explicitly for the well-studied nearby early-type disk galaxy NGC 2974 and found that a single component model overestimated the M/L by only 12%. This is not sufficient to explain the trends seen in Figure 7. Third, it is possible that the virial equation (2) for M/L_{vir} underestimates the true mass of rapidly rotating galaxies at high redshift. Rotation contributes to the hydrostatic support of the galaxy, so if it is ignored then the M/L will be underestimated. While rotation does increase σ_{eff} through the effect of line broadening, this may not fully capture the true hydrostatic importance of the rotation component. This may be especially important if the seeing is of order of or larger than the scale at which rotation is manifest. Such problems are avoided for local galaxies for which much higher quality data are available. This may explain the apparent differences between the M/L of rotating galaxies at low and high redshift. For our distant galaxies, correction formulae for $\sigma_{\text{eff}}/\sigma_c$ are used that are not themselves calibrated at high redshift.

5.2. Implications for the Evolution of M/L

In the previous section we demonstrated that M/L_{vir} may be too low for rapidly rotating galaxies at higher redshifts, but not for local early-type galaxies. Since the fundamental plane is in essence a correlation between M/L_{vir} and other global galaxy parameters, this will bias the amount of M/L evolution inferred from fundamental plane studies (see van Dokkum & van der Marel 2007, and references therein). van der Wel et al. (2005) found that the rate of luminosity evolution for the sam-

ple of field galaxies that we also use in this paper is $\Delta \log(M/L) = (-0.76 \pm 0.07)z$. Figures 6 and 7 suggest that, averaged over the rotating and non-rotating galaxies in our sample, M/L_{vir} may be too low by $\sim 20\%$. If so, then the evolution in M/L is reduced to $\log(M/L) = (-0.69 \pm 0.07)z$. This is steeper than the evolution found for cluster galaxies, but not by much (van Dokkum & van der Marel 2007).

The difference between M/L_{Jeans} and M/L_{vir} depends on the galaxy rotation rate. Moreover, rotating galaxies tend to have smaller R_{eff} than non-rotating galaxies (see Figure 7c). Therefore, our results also have consequences for the measured evolution of the tilt of the fundamental plane, and hence for the slope in the relation between M/L and either M or σ (as discussed previously by van der Marel & van Dokkum (2007b)). Evolution in the tilt of the fundamental plane has been observed by many authors (van der Wel et al. 2004; Treu et al. 2005; van der Wel et al. 2005; di Serego Alighieri et al. 2005; Jørgensen et al. 2005). However, it is a matter of debate to what extent sample selection effects contribute to the observed evolution (van der Wel et al. 2005; Treu et al. 2005). To illustrate the consequences of the results presented in this paper we revisit the analysis from van der Wel et al. (2005). They showed that the probability that the observed distribution of M_{vir} and M/L_{vir} is drawn from a parent population with the same distribution as the local galaxy population, apart from a constant amount of luminosity evolution inferred from the most massive galaxies, is as low as 0.14%. We repeat the analysis but now using the distribution of M_{Jeans} and M/L_{Jeans} , and find that this increases the probability to 3.0%. In other words, the evidence for mass-dependent evolution of M/L remains strong, but it does become weaker.

These arguments illustrate that the often observed evolution of the tilt of the fundamental plane is not necessar-

ily entirely due to mass-dependent evolution of the M/L , i.e., down-sizing. In order to determine to what extent the slope and the scatter of the relation between M/L and M evolve, still deeper observations are required to overcome the biases caused by sample selection effects in the surveys conducted over the past few years. In addition, it may be necessary to use dynamical modeling, as we do in this paper, to overcome the shortcomings of virial and fundamental plane mass estimates.

6. CONCLUSIONS

We use the spatial information of our previously published VLT/FORS2 absorption line spectroscopy to measure mean stellar velocity and velocity dispersion profiles of 25 field early-type galaxies in the redshift range $0.6 < z < 1.2$, with median redshift $z = 0.97$. The kinematical profiles can be reliably measured even in the most distant galaxies. Rotation is detected in the majority of the sample. Surface brightness profiles are determined from HST imaging. Two-integral solutions of the Jeans equations for oblate axisymmetric, constant axial-ratio models are calculated to interpret the data, taking into account line-of-sight projection, seeing convolution, and pixel/slit binning. This yields for each galaxy the degree of rotational support, as quantified by the parameter k , and the mass-to-light ratio M/L_{Jeans} (van der Marel & van Dokkum 2007a).

The rapidly-rotating ($k \gtrsim 0.6$) and slow-rotating ($k \lesssim 0.6$) galaxies in the distant sample tend to have different global properties. The rapidly-rotating galaxies tend to have later morphological types (S0 or Sa) and tend to be less luminous and more elongated. The slow-rotating galaxies tend to have earlier morphological types (E) and tend to be more luminous and rounder. The systematic variations with luminosity and axial ratio suggest that the correlation with morphological type is real, in agreement with the findings of Moran et al. (2007). Local E and S0 galaxies show a more complex and overlapping set of kinematic properties (e.g., Cappellari et al. 2007). The contrasting clean separation of rotating and non-rotating galaxies according morphological type observed at $z \sim 1$ is most likely partially artificial and must be related to the fact that round/face-on S0 galaxies are often misclassified as E galaxies, at high redshift even more so than at low redshift.

We have compiled a local comparison sample to study evolution of the field early-type (E+S0) galaxy rotation

rate. The distribution of k in our $z \sim 1$ sample is statistically indistinguishable from the distribution of $(V/\sigma)^*$, a comparable measure of rotational support, in the local sample. The relative fraction of rotating galaxies does not change significantly between $z \sim 1$ ($63 \pm 11\%$) and the present ($61 \pm 5\%$). If rotation is taken to be a reliable indicator of morphological type, then this provides evidence for an unchanging fraction of S0 galaxies in the early-type field galaxy population with redshift. This conflicts with the findings of (Moran et al. 2007) who did not correct for the effects of seeing convolution and pixel/slit binning on the measured rotation curves. It is possible that this may have led to an underestimate of the number of rapidly rotating field galaxies at $z \sim 0.5$ in their study.

We have compared the mass-to-light ratio M/L_{Jeans} from our spatially resolved models to the values M/L_{vir} inferred by applying the virial theorem to globally averaged quantities. For E galaxies, which are generally slow-rotating, we find good agreement using a homology parameter $\beta = 5$, which is consistent with the value calibrated locally. So there is no evidence for non-homologous evolution of E galaxies out to $z \sim 1$. On the other hand, for elongated, rotating galaxies (which are often S0s) we find that M/L_{Jeans} is on average $\sim 40\%$ higher than M/L_{vir} (see Figs. 6 and 7). For local galaxies this trend is not observed. This may hint at non-homologous evolution of this galaxy population (β increasing with redshift); it may suggest that our dynamical models produce biased results in these galaxies because of the neglect of cold disks; or it may suggest that the virial formula for M/L produces biased results when applied to poorly resolved, rapidly rotating galaxies at high redshift. We cannot unambiguously identify the true cause, but to us the latter seems to be the most straightforward explanation. If so, then studies of fundamental plane evolution overestimate both the amount of evolution, as well as the evolution in the tilt of the fundamental plane (and the relation between M and M/L), which is generally interpreted as evidence of down-sizing.

The authors would like to thank Pieter van Dokkum, Marijn Franx, Michele Cappellari, Dan Kelson, and Stijn Wuyts for helpful discussions and suggestions. A.v.d.W. acknowledges support from NASA grant NAG5-7697.

REFERENCES

- Bekki, K. 1997, ApJ, 490, L37
 Bell, E. F. et al. 2004, ApJ, 608, 752
 Binney, J. 1978, MNRAS, 183, 501
 Blakeslee, J. P. et al. 2003, ApJ, 596, L143
 Brown, M. J. I. et al. 2007, ApJ, 654, 858
 Cappellari, M. et al. 2006, MNRAS, 366, 1126
 Cappellari, M. et al. 2007, MNRAS, 379, 418
 Cinzano, P., & van der Marel, R. P. 1994, MNRAS, 270, 325
 Davies, R. L., Efstathiou, G., Fall, S. M., Illingworth, G., & Schechter, P. L. 1983, ApJ, 266, 41
 di Serego Alighieri, S. et al. 2005, A&A, 442, 125
 Dressler, A. et al. 1997, ApJ, 490, 577
 Emsellem, E. et al. 2007, MNRAS, 379, 401
 Giavalisco, M. et al. 2004, ApJ, 600, L93
 Gunn, J. E., & Gott, J. R. 1972, ApJ, 176, 1
 Holden, B. P. et al. 2007, ApJ, 670, 195
 Jørgensen, I., Franx, M., & Kjaergaard, P. 1995b, MNRAS, 276, 1341
 Jørgensen, I., Bergmann, M., Davies, R., Barr, J., Takamiya, M., & Crampton, D. 2005, AJ, 129, 1249
 Kronawitter, A., Saglia, R. P., Gerhard, O., & Bender, R. 2000, A&AS, 144, 53
 Koopmans, L. V. E., Treu, T., Bolton, A. S., Burles, S., & Moustakas, L. A. 2006, ApJ, 649, 599
 Larson, R. B., Tinsley, B. M., & Caldwell, C. N. 1980, ApJ, 237, 692
 Le Floch, E. et al. 2005, ApJ, 632, 169
 Moran, S. M., Loh, B. L., Ellis, R. S., Treu, T., Bundy, K., & MacArthur, L. A. 2007, ApJ, 665, 1067
 Naab, T., Jesseit, R., & Burkert, A. 2006a, MNRAS, 372, 839
 Naab, T., Khochfar, S., & Burkert, A. 2006b, ApJ, 636, L81
 Noeske, K. G. et al. 2007, ApJ, 660, L43
 Paturel, G. et al. 1997, A&AS, 124, 109

- Paturel, G. et al. 2003, A&A, 412, 45
Postman, M. et al. 2005, ApJ, 623, 721
Prugniel, P., & Simien, F. 1996, A&A, 309, 749
Richstone, D. O., Bower, G., & Dressler, A. 1990, ApJ, 353, 118
Rix, H.-W., & White, S. D. M. 1990, ApJ, 362, 52
Smith, G. P., Treu, T., Ellis, R. S., Moran, S. M., & Dressler, A. 2005, ApJ, 620, 78
Treu, T. et al. 2005, ApJ, 633, 174
van der Marel, R. P. 1991, MNRAS, 253, 710
van der Marel, R. P., Cretton, N., de Zeeuw, P. T., & Rix, H.-W. 1998, ApJ, 493, 613
van der Marel, R. P., & van Dokkum, P. G. 2007a, ApJ, 668, 738
—. 2007b, ApJ, 668, 756
van der Wel, A., Franx, M., van Dokkum, P. G., & Rix, H.-W. 2004, ApJ, 601, L5
van der Wel, A., Franx, M., van Dokkum, P. G., Rix, H.-W., Illingworth, G. D., & Rosati, P. 2005, ApJ, 631, 145
van der Wel, A. et al. 2007, ApJ, 670, 206
van Dokkum, P. G., & van der Marel, R. P. 2007, ApJ, 655, 30
Verolme, E. K. et al. 2002, MNRAS, 335, 517